

The roles of *Fgf4* and *Fgf8* in limb bud initiation and outgrowth

Anne M. Boulet^a, Anne M. Moon^{b,c}, Benjamin R. Arenkiel^a, Mario R. Capecchi^{a,*}

^aDepartment of Human Genetics, Howard Hughes Medical Institute, University of Utah School of Medicine, Salt Lake City, UT 84112, USA

^bProgram in Human Molecular Biology and Genetics, University of Utah School of Medicine, Salt Lake City, UT 84112, USA

^cDepartment of Pediatrics, University of Utah School of Medicine, Salt Lake City, UT 84112, USA

Received for publication 12 May 2004, revised 16 June 2004, accepted 21 June 2004

Abstract

Although numerous molecules required for limb bud formation have recently been identified, the molecular pathways that initiate this process and ensure that limb formation occurs at specific axial positions have yet to be fully elucidated. Based on experiments in the chick, *Fgf8* expression in the intermediate mesoderm (IM) has been proposed to play a critical role in the initiation of limb bud outgrowth via restriction of *Fgf10* expression to the appropriate region of the lateral plate mesoderm. Contrary to the outcome predicted by this model, ablation of *Fgf8* expression in the intermediate mesoderm before limb bud initiation had no effect on initial limb bud outgrowth or on the formation of normal limbs. When their expression patterns were first elucidated, both *Fgf4* and *Fgf8* were proposed to mediate critical functions of the apical ectodermal ridge (AER), which is required for proper limb bud outgrowth. Although mice lacking *Fgf4* in the AER have normal limbs, limb development is severely affected in *Fgf8* mutants and certain skeletal elements are not produced. By creating mice lacking both *Fgf4* and *Fgf8* function in the forelimb AER, we show that limb bud mesenchyme fails to survive in the absence of both FGF family members. Thus, *Fgf4* is responsible for the partial compensation of distal limb development in the absence of *Fgf8*. A prolonged period of increased apoptosis, beginning at 10 days of gestation in a proximal–dorsal region of the limb bud, leads to the elimination of enough mesenchymal cells to preclude formation of distal limb structures. Expression of *Shh* and *Fgf10* is nearly abolished in double mutant limb buds. By using a CRE driver expressed in both forelimb and hindlimb ectoderm to inactivate *Fgf4* and *Fgf8*, we have produced mice lacking all limbs, allowing a direct comparison of FGF requirements in the two locations.

© 2004 Elsevier Inc. All rights reserved.

Keywords: FGF; Limb development; Mouse; Intermediate mesoderm; Limb bud initiation; Apical ectodermal ridge; Cell survival; Apoptosis

Introduction

Numerous factors have been proposed to be required for the processes of limb bud initiation and outgrowth in the mouse and in the chick (Johnson and Tabin, 1997; Martin, 1998). Recent gene knockout experiments in the mouse have confirmed the importance of some of these molecules and have identified others with unexpected functional roles (Niswander, 2003; Tickle, 2003; Tickle and Munsterberg,

2001). Due to their localization in the apical ectodermal ridge (AER), a structure that plays a critical role in maintenance of limb bud development, members of the FGF family were proposed to be involved in the control of limb bud outgrowth and patterning. Moreover, experiments in the chick demonstrated that FGFs could indeed substitute for the AER (Crossley et al., 1996; Fallon et al., 1994; Niswander et al., 1993).

Fgf8 is expressed in the ventral limb ectoderm when the limb bud can first be detected, before the appearance of transcripts for any other FGF family member, and is subsequently expressed throughout the AER. Expression of *Fgf8* has also been detected in the intermediate mesoderm (IM) of both chick and mouse embryos before limb bud initiation (Agarwal et al., 2003; Crossley et al., 1996; Vogel et

* Corresponding author. Department of Human Genetics, Howard Hughes Medical Institute, University of Utah School of Medicine, 15 North 2030 East, Suite 5400, Salt Lake City, UT 84112-5331. Fax: +1 801 585 3425.

E-mail address: mario.capecchi@genetics.utah.edu (M.R. Capecchi).

al., 1996). Studies in the chick system have pointed to the IM as a potential source of the endogenous limb bud inducer (Martin, 1998). When the mesonephros is ablated or when communication between the mesonephros and the lateral plate mesoderm is blocked, wing development is severely affected (Geduspan and Solursh, 1992; Stephens and McNulty, 1981; Stephens et al., 1993). These studies suggested a model in which a signal from the IM or mesonephros is required to initiate limb bud formation. *Fgf8* expression in the IM of the chick correlates spatially and temporally with limb bud initiation from the lateral plate mesoderm. Based on expression of *Fgf8* in the IM at the appropriate developmental time, FGF8 became the favorite candidate for such an inducer (Crossley et al., 1996; Vogel et al., 1996). Specifically, *Fgf8* has been proposed to be required for restriction of *Fgf10* to the limb bud-forming region of the lateral plate mesoderm (Ohuchi et al., 1997), and FGF8 induction of *Fgf10* is thought to be mediated by WNT2b signaling in the chick (Kawakami et al., 2001). Therefore, because *Fgf10* is absolutely required for limb bud outgrowth (Min et al., 1998; Sekine et al., 1999), the model predicts that *Fgf8* is essential for initiation or positioning of the forelimb bud as the first step in the cascade. Although it is often cited in the literature, not all experimental evidence supports this model (Fernandez-Teran et al., 1997).

The role of *Fgf8* expressed in the AER in the maintenance of limb bud outgrowth has been well established (Lewandoski et al., 2000; Moon and Capecchi, 2000). Interestingly, although limb development is abnormal in mouse embryos lacking *Fgf8* expression in the forelimb AER, limb bud outgrowth nevertheless continues and the ulna and four digits are formed in a relatively normal manner (Moon and Capecchi, 2000). Similar findings are obtained when *Fgf8* expression is ablated from the hindlimb AER (Lewandoski et al., 2000). The sustained development of distal limb elements suggests that the loss of *Fgf8* expression is partially compensated by the activity of another FGF family member in the AER.

Mice lacking limb expression of *Fgf4* have normal forelimbs and hindlimbs (Moon et al., 2000; Sun and Martin, 2000). Nevertheless, the ability of *Fgf4* to provide AER function in in vitro assays and the observation that *Fgf4* expression is altered in *Fgf8* limb mutants suggest that it may compensate for the lack of *Fgf8*. The fact that production of FGF4 by the AER is delayed relative to FGF8 by approximately 1 day readily explains the failure to rescue development of the humerus or the femur. This prediction has been tested for the hindlimb, demonstrating that outgrowth and skeletal development fail in the absence of both *Fgf4* and *Fgf8* (Sun et al., 2002). However, forelimb expression of *Fgf8* and *Fgf4* was not completely ablated in this system, and elements of all three segments of the forelimb skeleton were still present. Thus, the characteristics of the CRE driver used in these experiments precluded a comprehensive evaluation of the roles of FGF4 and FGF8 in forelimb development (Sun et al., 2002).

In this manuscript, we investigate the various roles suggested for *Fgf4* and *Fgf8* in mouse limb bud outgrowth. To determine whether *Fgf8* is required for limb bud initiation, we have eliminated expression of *Fgf8* in the IM. To test the hypothesis that the formation of distal forelimb structures in *Fgf8* conditional limb mutants is due to compensation by *Fgf4*, we produced mice that lack expression of both *Fgf4* and *Fgf8* in the forelimb. More importantly, we show that production of CRE from the AP2 α locus (*AP2-Cre*) results in recombination-mediated inactivation of *Fgf4* and *Fgf8* in both forelimb and hindlimb ectoderm. Finally, utilization of the *AP2-Cre* driver has allowed us to address the question of differences in FGF requirement in formation of forelimb versus hindlimb.

Materials and methods

Generation and genotyping of mutant mice

The *Fgf4* alleles used to generate double mutant mice were the *Fgf4* conditional allele (*Fgf4^{AP}*) described previously (Moon et al., 2000) and a “minimal” *Fgf4* conditional allele lacking both the human placental alkaline phosphatase (PLAP) reporter and the NEO gene (*Fgf4^{FRT}*). Both are referred to interchangeably as *Fgf4^c* (*Fgf4* conditional). The *Fgf8* conditional alleles (*Fgf8^{AP}* and *Fgf8^{GFP}*, called *Fgf8^c*) were described previously (Macatee et al., 2003; Moon and Capecchi, 2000). The *RAR-Cre* driver and the *AP2-Cre* driver were previously described (Moon et al., 2000; Macatee et al., 2003; Arenkiel et al., 2004).

The *Lefty2-Cre* transgene was constructed by placing the 5.5 kb *Lefty2* promoter fragment that was shown to reproduce the expression pattern of the endogenous gene (Saijoh et al., 1999) upstream of coding sequences for CRE recombinase (Sauer and Henderson, 1988).

Immunofluorescence on cryosections and whole embryos

Frozen 10 μ m sections of mutant and control embryos were subjected to the TUNEL reaction using the In Situ Cell Death Detection Kit (TMR red, Roche), or stained with anti-pHH3 (anti-phospho-Histone H3, rabbit IgG, Upstate Biotechnology), anti-Sox10/9 (kindly provided by M. Wegner), or anti-cleaved Caspase-3 (rabbit anti-cleaved Caspase-3 (Asp175), Cell Signaling Technology) antibodies. The anti-Sox10/9 monoclonal antibody was generated against Sox10, but cross-reacts with Sox9. Primary antibodies were detected with goat anti-mouse or anti-rabbit Alexa Fluor 488 or 594 antibodies (Molecular Probes).

For whole mount staining of embryos, an anti-GFP primary antibody (rabbit anti-green fluorescent protein, Molecular Probes) and a goat anti-rabbit secondary antibody (Alexa Fluor 488, Molecular Probes) were used.

Images were captured on a BIORAD confocal microscope.

Whole mount in situ hybridization and staining for β -Gal and alkaline phosphatase

Whole mount in situ hybridization was carried out as described (Boulet and Capecchi, 1996). The *Fgf10* probe was obtained from D. Ornitz and C. Deng, and the *Shh* probe was provided by A. McMahon. The *Sox9* probe was described previously (Boulet and Capecchi, 2004).

Staining for human placental alkaline phosphatase and β -Gal was performed as previously described (Moon et al., 2000).

Skeletal analysis

Alcian blue staining of E13–13.5 embryos followed the protocol described in Wanek et al. (1989), except that

embryos were cleared in 90% glycerol after staining. Newborn skeleton preparations were carried out as described (Boulet and Capecchi, 2004).

Results

Fgf8 is not required for initial limb bud outgrowth

Fgf8 expression is readily detectable in the IM of chick embryos between stages 13 and 15 (Crossley et al., 1996; Vogel et al., 1996). Although the initial study of the mouse *Fgf8* gene reported expression in the nephrogenic cords only at E9.5–E10 (Crossley and Martin, 1995), the presence of *Fgf8* transcripts in the IM at an earlier stage, before limb bud outgrowth (E8.5 to E9.25), has recently

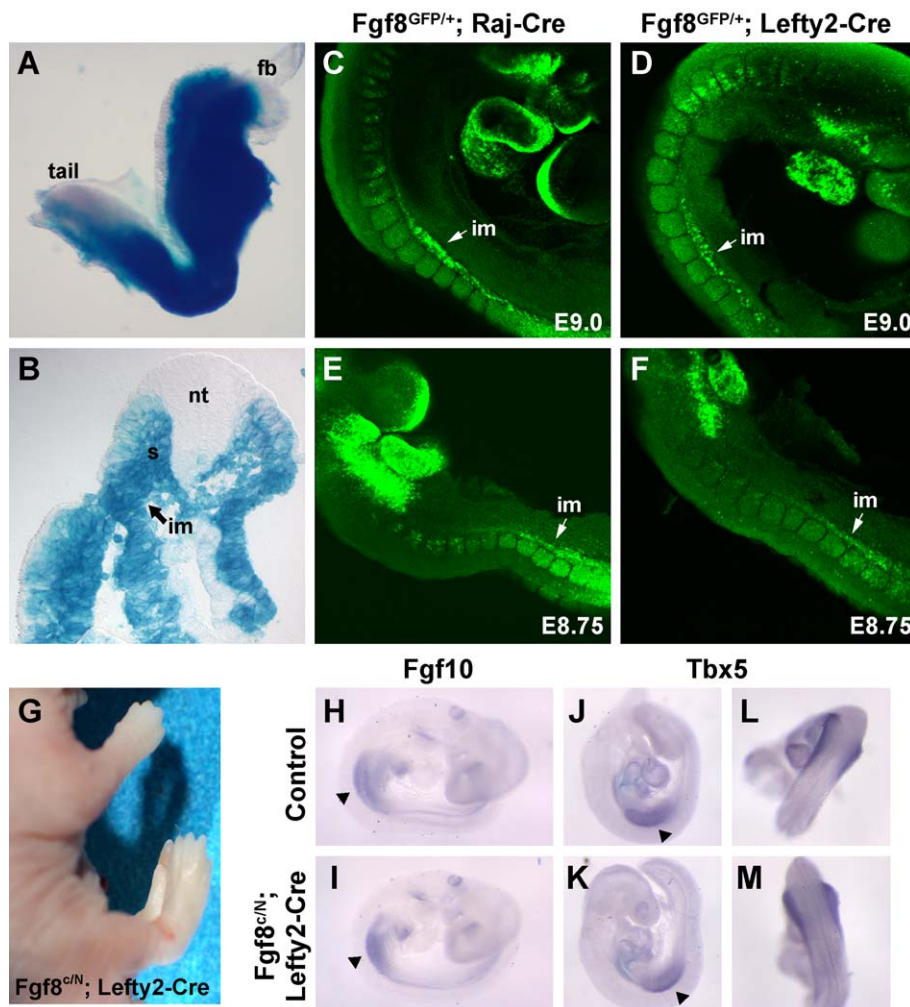


Fig. 1. CRE-mediated inactivation of *Fgf8* in the intermediate mesoderm. (A) β -Galactosidase expression shows that the *Lefty2-Cre* transgene mediates recombination of the R26R reporter throughout the mesoderm at E8.75. fb, forebrain. (B) Section through an E9.25 embryo showing *Lefty2-Cre*-mediated recombination of R26R in the intermediate mesoderm (im) and somitic mesoderm (s), but not in the neural tube (nt). (C and E) GFP expression from the *Fgf8* locus activated by ubiquitously expressed *Raj-Cre* at E9.0 (C) and E8.75 (E). GFP expression, detected with the anti-GFP antibody, reproduces the *Fgf8* expression pattern. (D and F) GFP expression from the *Fgf8* locus after CRE-mediated recombination using the *Lefty2-Cre* transgene at E9.0 (D) and E8.75 (F). Staining is only seen where *Fgf8* and *Lefty2-Cre* patterns overlap. (G) *Fgf8*^{c/N}; *Lefty2-Cre* newborn. Limbs are completely normal. (H) Expression of *Fgf10* in a control E9.5 embryo. (I) Expression of *Fgf10* in an *Fgf8*^{c/N}; *Lefty2-Cre* embryo at E9.5. (J–M) Expression of *Tbx5* in control E9.5 (J and L) and *Fgf8*^{c/N}; *Lefty2-Cre* E9.5 (K and M) embryos. Arrowheads mark forelimb bud expression of *Fgf10* and *Tbx5*.

been confirmed in mouse embryos (Agarwal et al., 2003). To decisively establish whether *Fgf8* plays any role in limb bud initiation, we have inactivated *Fgf8* using a Cre driver expressed in the IM.

Because detection of *Fgf8* transcripts in the IM of mouse embryos by whole mount in situ hybridization is unreliable, we visualized *Fgf8* gene expression using the *Fgf8*^{GFP} allele (Macatee et al., 2003). In this allele, expression of GFP occurs only in cells in which the *Fgf8* promoter is active and CRE has induced recombination between the two loxP sites, thereby inactivating the gene. When ubiquitously expressed Cre recombinase (*Raj-Cre*) (Schwenk et al., 1995) was used, GFP expression was clearly present in the IM of embryos at E8.75 to E9.0 (Figs. 1C and E). To inactivate *Fgf8* in the IM, we employed a *Lefty2-Cre* transgene. Examination of the *Lefty2-Cre* expression pattern using the ROSA26-β-Gal reporter line (R26R) (Soriano, 1999) shows that CRE is active throughout the mesoderm during the desired developmental window (Figs. 1A and B). Although *Lefty2* is

known as a gene whose expression is restricted to the left side of the early embryo, *Lefty2* transcripts are initially detected in mesoderm emerging from the primitive streak (at E7.0) with no apparent left–right asymmetry (Meno et al., 1997). This aspect of *Lefty2* gene expression is likely to explain the observed lineage pattern of cells that have undergone Cre-mediated recombination. The presence of extensive GFP expression in the IM from the *Fgf8*^{GFP} allele after recombination by *Lefty2-Cre* confirmed that the *Fgf8* locus was inactivated in the appropriate cells at the appropriate time (Figs. 1D and F). In spite of *Fgf8* inactivation in the IM by *Lefty2-Cre*, the position and timing of forelimb bud initiation were completely unaffected and limb bud development proceeded normally (Fig. 1G). To ensure that roles proposed for *Fgf8* in the IM were carried out in its absence, *Fgf8*^{cN}; *Lefty2-Cre* embryos were examined for *Tbx5* and *Fgf10* expression. Expression patterns of both critical genes were indistinguishable from those of control embryos (Figs. 1H–M).

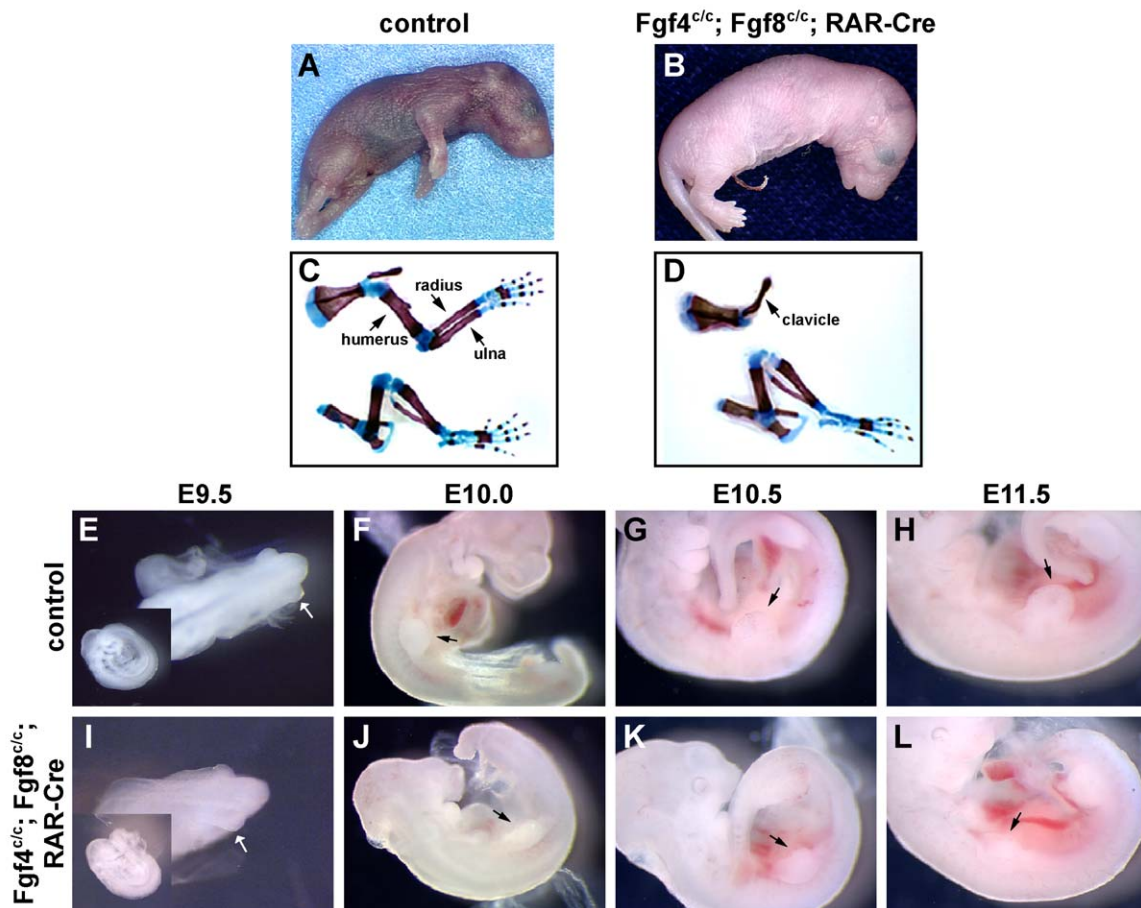


Fig. 2. Forelimbs are absent when both *Fgf4* and *Fgf8* are inactivated using *RAR-Cre*, although forelimb bud initiation is normal. (A) Control newborn. (B) *Fgf4*^{c/c}; *Fgf8*^{c/c}; *RAR-Cre* mutant newborn. Limb skeleton preparations of (C) control and (D) *Fgf4*^{c/c}; *Fgf8*^{c/c}; *RAR-Cre* newborns. (E–H) Control embryos at E9.5 (E, inset shows lateral view of same embryo), E10.0 (F), E10.5 (G), and E11.5 (H) showing normal forelimb bud outgrowth (arrows). (I–L) *Fgf4*^{c/c}; *Fgf8*^{c/c}; *RAR-Cre* double mutants at E9.5 (I, inset shows lateral view of same embryo), E10.0 (J), E10.5 (K), and E11.5 (L) with normal limb bud initiation, but no further forelimb bud outgrowth (arrows).

Inactivation of Fgf4 and Fgf8 by RAR-Cre leads to the complete absence of forelimbs in newborns

Although elimination of *Fgf8* expression from the forelimb AER using an *RAR-Cre* transgene causes severe defects in the forelimb skeleton, the most distal limb elements are still formed (Moon and Capecchi, 2000). Expression of other FGF family members in the AER may allow continued limb outgrowth in the absence of *Fgf8*. When both *Fgf4* and *Fgf8* genes were inactivated using *RAR-Cre*, newborns completely lacked forelimbs (Figs. 2A and B). The scapula was present, but none of the distal skeletal elements were formed (Figs. 2C and D). Because expression of *RAR-Cre* does not encompass the entire posterior limb field (Moon et al., 2000), as expected, the only defect seen in the hindlimbs of *RAR-Cre* double mutants was the loss of digit 1 (Figs. 2C and D).

Although *Fgf4^{c/c}; Fgf8^{c/c}; RAR-Cre* newborns completely lacked forelimbs, double mutant embryos at E9.5 showed normal limb bud initiation (Figs. 2E and I). However, by E10.0, when control littermates had forelimb buds at stage 2 (Wanek et al., 1989), double mutant forelimbs were noticeably smaller than control forelimbs (Figs. 2F and J). The difference in forelimb bud size was even more striking at E10.5 (Figs. 2G and K). By 11.5, the double mutant forelimbs were just a fraction of the size of control forelimbs (Figs. 2H and L). Although a small forelimb bud still protruded from the body wall at E13, no Alcian blue staining was detectable distal to the scapula (Figs. 3A and

E), while *Fgf4^{c/+}; Fgf8^{c/c}; RAR-Cre* specimens and *Fgf8^{c/c}; RAR-Cre* single mutants show staining of the ulna by this stage (Fig. 3C, data not shown). In *RAR-Cre*-generated mutants, Alcian blue staining of hindlimb stylopod and zeugopod cartilage is not significantly different from that of control (Figs. 3B, D, and F).

Inactivation of Fgf4 and Fgf8 with AP2-Cre results in the absence of both forelimbs and hindlimbs

To inactivate *Fgf4* and *Fgf8* in the ectoderm of both forelimbs and hindlimbs, we utilized an *AP2-Cre* line (Macatee et al., 2003). β -Gal staining of embryos from matings of *AP2-Cre* males to *ROSA26* (*R26R*) females (Soriano, 1999) showed that CRE recombinase was present in the limb bud ectoderm of E9.5 embryos (Macatee et al., 2003). To directly determine the temporal and spatial characteristics of *AP2-Cre*-mediated recombination at the *Fgf8* locus, *AP2-Cre* males were mated to females carrying conditional alleles of *Fgf8* designed for CRE-inducible expression of either human placental alkaline phosphatase (PLAP) (Moon and Capecchi, 2000) or GFP (Macatee et al., 2003). With the GFP or PLAP conditional alleles, the *Fgf8* gene is inactivated wherever CRE is present, while the reporter will only be activated in sites where both CRE and *Fgf8* are expressed (Macatee et al., 2003; Moon and Capecchi, 2000). GFP produced from recombination of the *Fgf8^{GFP}* allele by *AP2-Cre* was detected in the forelimb bud ventral ectoderm when the bud is first discernible (Fig. 4A). Similarly, PLAP expression was detected in *Fgf8^{AP/+}*;

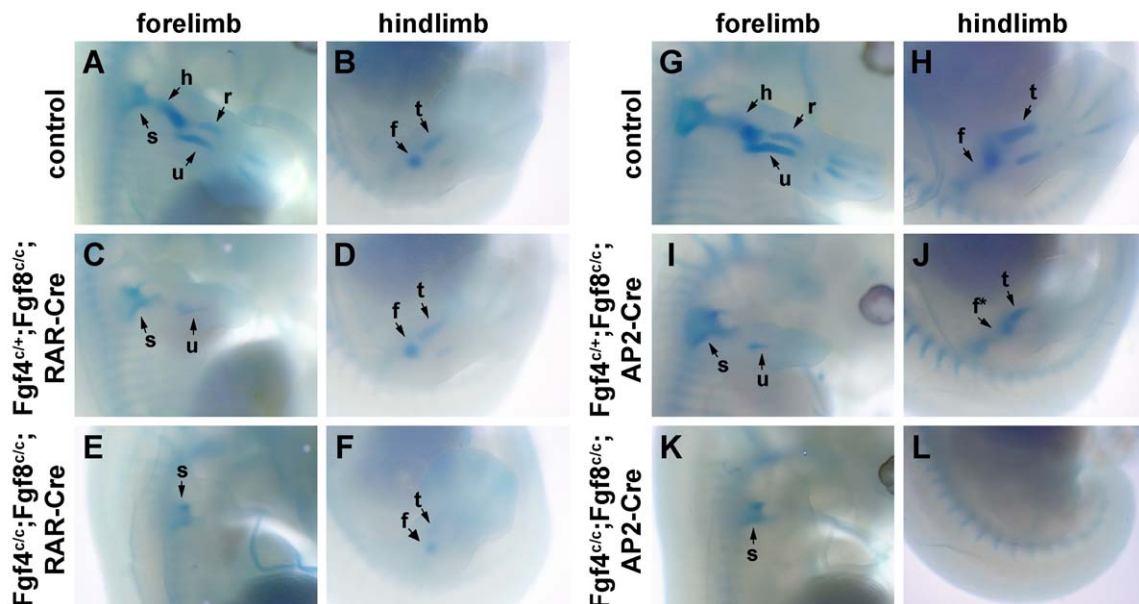


Fig. 3. Alcian blue staining of cartilage elements in control and mutant limbs. (A) Control E13 forelimb. (B) Control E13 hindlimb. (C and D) *Fgf4^{c/+}; Fgf8^{c/c}; RAR-Cre* E13 mutant forelimb and hindlimb. No differences were detected between *Fgf4^{c/+}; Fgf8^{c/c}; RAR-Cre* and *Fgf4^{+/+}; Fgf8^{c/c}; RAR-Cre* specimens. (E and F) *Fgf4^{c/c}; Fgf8^{c/c}; RAR-Cre* E13 double mutant forelimb and hindlimb. (G and H) Control E13.5 forelimb and hindlimb. (I and J) *Fgf4^{c/+}; Fgf8^{c/c}; AP2-Cre* E13.5 forelimb and hindlimb. (K and L) *Fgf4^{c/c}; Fgf8^{c/c}; AP2-Cre* E13.5 double mutant forelimb and hindlimb. s, scapula; h, humerus; r, radius; u, ulna; f, femur; f*, femur remnant; t, tibia. No differences in limb development were detected between *Fgf4^{+/+}; Fgf8^{c/c}; AP2-Cre* and *Fgf4^{c/+}; Fgf8^{c/c}; AP2-Cre* specimens.

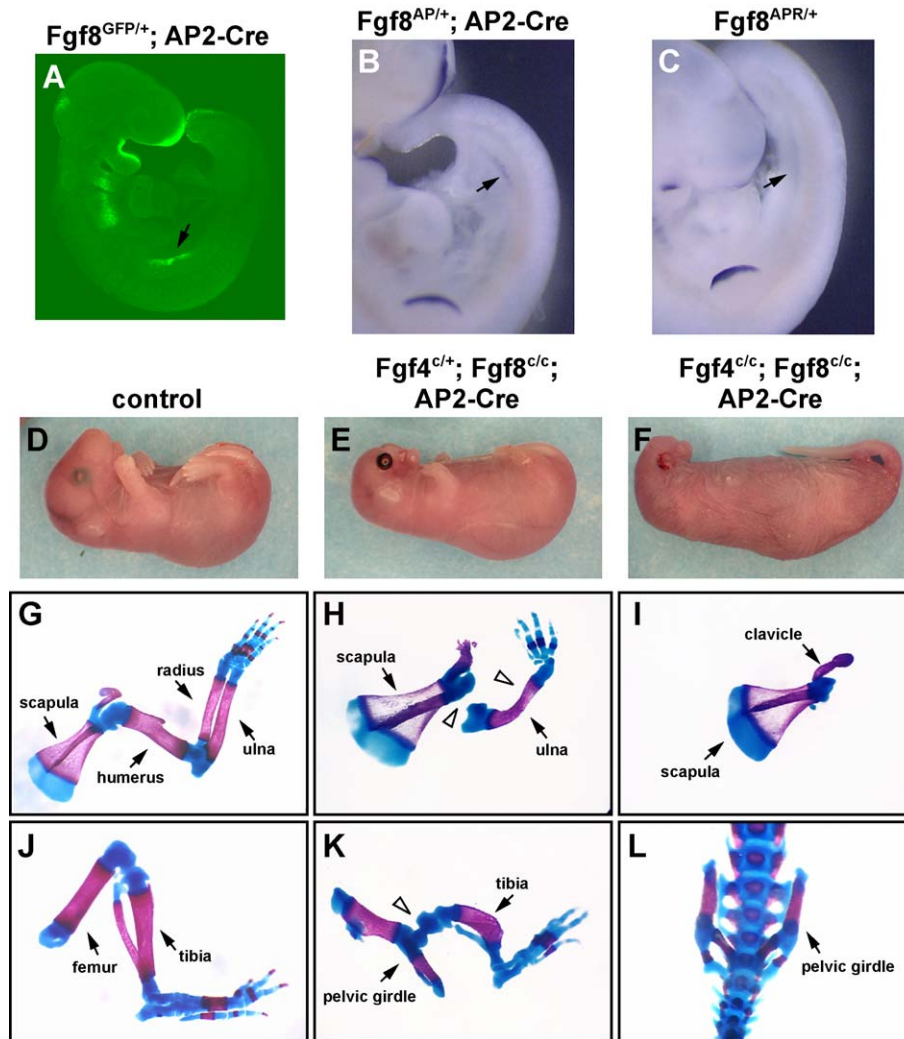


Fig. 4. Inactivation of *Fgf4* and *Fgf8* in both forelimb and hindlimb by *AP2-Cre* causes failure of forelimb and hindlimb outgrowth. (A) *Fgf8^{GFP/+}; AP2-Cre* E9.5 embryo stained with an anti-GFP antibody showing CRE-mediated recombination, detected by induction of GFP expression, in early forelimb bud ventral ectoderm (arrow). (B) E10 embryo showing PLAP activity dependent upon *AP2-Cre*-mediated recombination at the *Fgf8* locus in the early hindlimb bud (arrow). (C) Embryo at E10 in which PLAP activity is derived from an *Fgf8^{AP}* allele recombined in the germ line (i.e., CRE independent). Expression of PLAP in the hindlimb (arrow) directly reflects *Fgf8* transcription. (D) Control newborn mouse. (E) *Fgf4^{c/+}; Fgf8^{c/c}; AP2-Cre* newborn. (F) *Fgf4^{c/c}; Fgf8^{c/c}; AP2-Cre* newborn. Newborn skeleton preparations of (G) control forelimb, (H) *Fgf4^{c/+}; Fgf8^{c/c}; AP2-Cre* forelimb, (I) *Fgf4^{c/c}; Fgf8^{c/c}; AP2-Cre* forelimb, (J) control hindlimb, (K) *Fgf4^{c/+}; Fgf8^{c/c}; AP2-Cre* hindlimb, and (L) *Fgf4^{c/c}; Fgf8^{c/c}; AP2-Cre* pelvic region. Open arrowheads denote the positions of missing skeletal elements.

AP2-Cre hindlimb buds as early as in embryos that inherit a recombined *Fgf8^{AP}* allele (*Fgf8^{APR}*) in which PLAP activity is detected in all sites of *Fgf8* expression (Figs. 4B and C). The observation that *Fgf8*-driven PLAP expression dependent upon *AP2-Cre*-mediated recombination is detected as early as endogenous expression from the *Fgf8* locus strongly suggests that the *Fgf8* gene is inactivated before its expression in the hindlimb bud ectoderm.

When *AP2-Cre* was used to inactivate conditional alleles of *Fgf8*, forelimbs of single mutant newborns resembled those of newborns in which *Fgf8* was inactivated using *RAR-Cre* (Fig. 4E, Moon and Capecchi, 2000), except that the humerus was never present (Fig. 4H, $n = 8$). In addition, the hindlimbs of *Fgf8^{c/c}; AP2-Cre* or *Fgf4^{c/+}; Fgf8^{c/c}; AP2-Cre*

newborns were noticeably affected, with drastic reductions of the femur (Figs. 4E and K, data not shown). The femur was essentially absent in 75% (9/12) of hindlimbs scored and significantly reduced in the remaining cases. In addition, the fibula was severely reduced in 11 of 12 hindlimbs examined while the tibia was mildly affected in every specimen. This hindlimb phenotype is more severe than that observed when conditional alleles of *Fgf8* were inactivated using *Msx2-Cre* (Lewandoski et al., 2000). In *Fgf8^{c/c}; AP2-Cre* or *Fgf4^{c/+}; Fgf8^{c/c}; AP2-Cre* specimens at E13.5, no trace of the humerus was detectable by Alcian blue staining in forelimbs (Figs. 3G and I, data not shown), while only a reduced femur and tibia were evident in hindlimbs (Figs. 3H and J). By E15.5, a small tibia and fibula were present, but the shaft of

the femur was completely absent in *Fgf8^{cc/c}; AP2-Cre* mutants (data not shown).

When both *Fgf4* and *Fgf8* were inactivated using *AP2-Cre*, both forelimbs and hindlimbs were absent from newborn specimens (Fig. 4F). In these mutants, no skeletal elements were detected distal to the scapula or the pelvis, respectively (Figs. 4I and L). As seen with inactivation using *RAR-Cre*, limb buds were present in early *AP2-Cre*-induced double mutant embryos, with obvious size reduction visible by E10–E10.5 (data not shown). At E13.5, no Alcian blue-staining cartilage precursors of the skeletal elements of the forelimb or the hindlimb were present (Figs. 3K and L).

Failure of limb bud outgrowth in Fgf4/Fgf8 double mutants correlates with excess apoptosis in proximal limb mesenchyme

When *Fgf8* is inactivated by *RAR-Cre*, increased apoptosis of proximal–dorsal mesenchyme is observed at

E10.0 (Moon and Capecchi, 2000). In contrast, excessive apoptotic cells were not detected in forelimb buds of E9.5 or E11.5 mutants. Loss of mesenchymal cells during this period of apoptosis apparently resulted in the loss of precursors for the humerus, radius, and digit 1.

As expected, increased apoptosis was also observed in *Fgf4^{cc/c}; Fgf8^{cc/c}; RAR-Cre* double mutant embryos on day 10 of gestation. However, the period of excessive cell death was extended in double mutants. Increased apoptosis was first detected at E10–E10.5 (Figs. 5A and B), and then persisted at E11 and E11.5 in the AER as well as in the proximal–dorsal region (Figs. 5C–F). pHH3 staining and BrdU incorporation indicate that cell proliferation in distal mesenchyme generally continues even in the absence of *Fgf4* and *Fgf8* in the AER (Figs. 5B, D, and F; data not shown).

A large increase in the number of TUNEL-positive cells was also detected in the forelimbs of *Fgf4^{cc/c}; Fgf8^{cc/c}; AP2-Cre* embryos at E10.5 and in hindlimbs at E11.5 (Figs. 5G

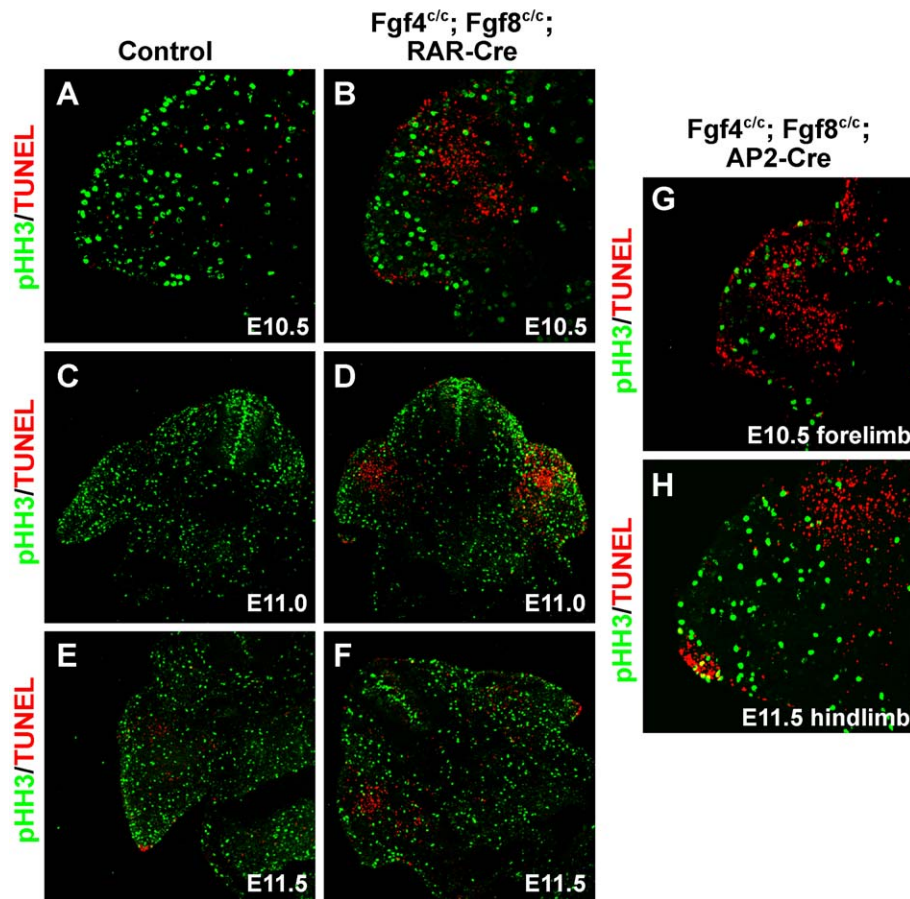


Fig. 5. Failure of limb outgrowth in embryos lacking *Fgf4* and *Fgf8* is due to excess apoptosis. TUNEL assay and phospho-histone H3 (pHH3) antibody staining of (A) control E10.5 forelimb, (B) E10.5 *Fgf4^{cc/c}; Fgf8^{cc/c}; RAR-Cre* forelimb, (C) E11.0 control forelimb region, (D) E11.0 *Fgf4^{cc/c}; Fgf8^{cc/c}; RAR-Cre* forelimbs, (E) forelimb region of E11.5 control embryo, (F) forelimbs of *Fgf4^{cc/c}; Fgf8^{cc/c}; RAR-Cre* E11.5 embryo, (G) forelimb of E10.5 *Fgf4^{cc/c}; Fgf8^{cc/c}; AP2-Cre* mutant embryo, and (H) hindlimb of E11.5 *Fgf4^{cc/c}; Fgf8^{cc/c}; AP2-Cre* mutant embryo. Images in A, B, G, and H were captured at 25 \times , and those shown in C, D, E, and F at 10 \times magnification.

and H). Because of the more severe phenotype with respect to the presence of the humerus in *AP2-Cre* compared to *RAR-Cre* specimens, we looked for increased apoptosis at E9.5 in both genotypes. Neither an increase in TUNEL-positive cells nor an increase in the number of activated Caspase-3-positive cells relative to controls could be detected at the earlier gestational time (data not shown).

Expression of Fgf10 and Shh are drastically reduced in double mutant limbs

Fgf8 and *Fgf4* have been proposed to be required for the maintenance of *Fgf10* expression in the distal limb bud mesenchyme. In *Fgf4/Fgf8* double mutants generated with *RAR-Cre*, *Fgf10* was detectable in the most distal portion of the forelimb bud at E10.5, albeit at a lower level than that

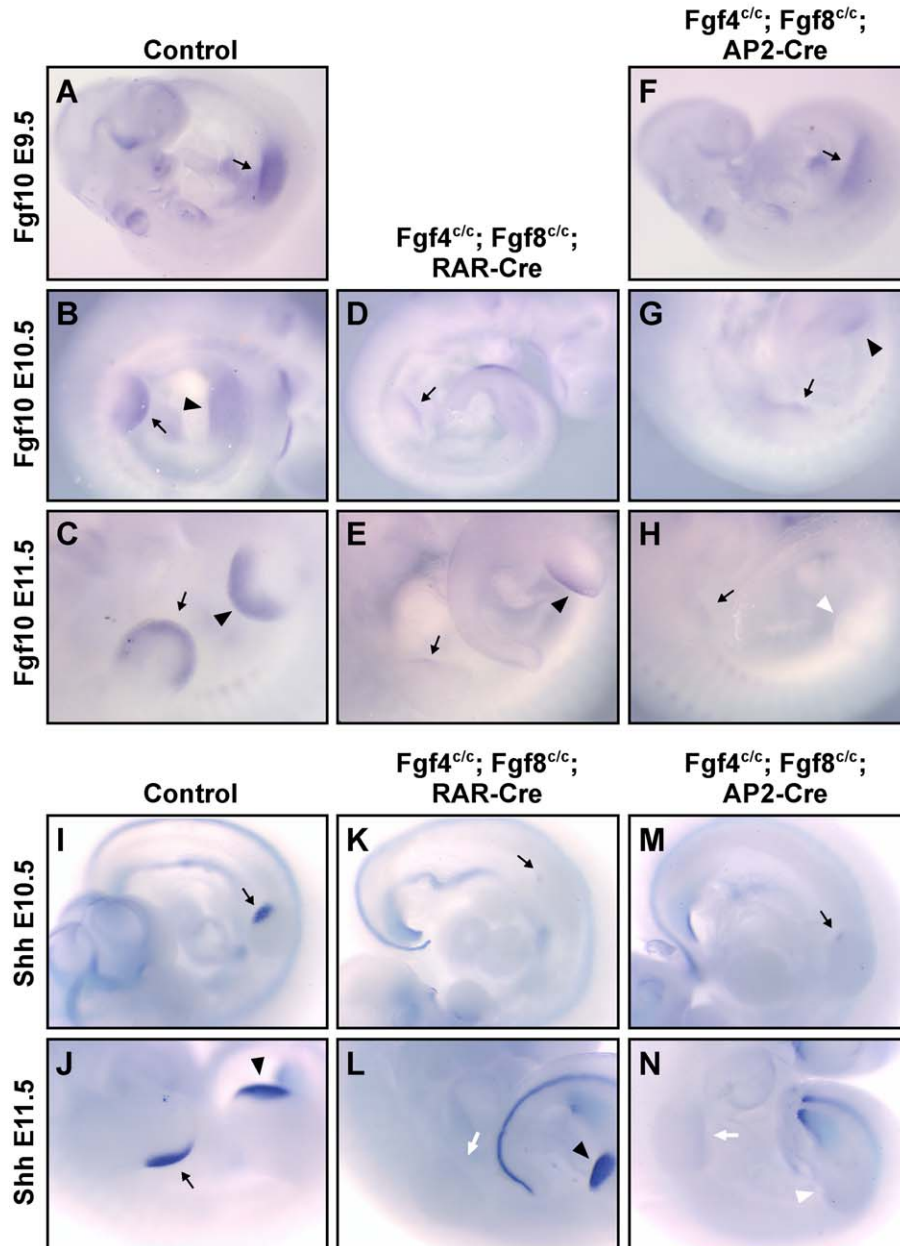


Fig. 6. Reduction or elimination of *Fgf10* and *Shh* expression in *Fgf4; Fgf8* double mutants. (A–H) Whole mount in situ hybridization with an *Fgf10* probe. Black arrows mark forelimbs and black arrowheads mark hindlimbs when visible. White arrows or arrowheads indicate absence of expression. (A) E9.5 control embryo, (B) E10.5 control, (C) E11.5 control, (D) E10.5 *Fgf4^{c/c}; Fgf8^{c/c}; RAR-Cre* embryo, (E) E11.5 *Fgf4^{c/c}; Fgf8^{c/c}; RAR-Cre*, (F) E9.5 *Fgf4^{c/c}; Fgf8^{c/c}; AP2-Cre* embryo, (G) E10.5 *Fgf4^{c/c}; Fgf8^{c/c}; AP2-Cre*, (H) E11.5 *Fgf4^{c/c}; Fgf8^{c/c}; AP2-Cre* embryo. (I–N) Whole mount in situ hybridization with a *Shh* probe. (I) E10.5 control, (J) E11.5 control embryo, (K) E10.5 *Fgf4^{c/c}; Fgf8^{c/c}; RAR-Cre* embryo, (L) E11.5 *Fgf4^{c/c}; Fgf8^{c/c}; RAR-Cre*, (M) E10.5 *Fgf4^{c/c}; Fgf8^{c/c}; AP2-Cre* embryo, and (N) E11.5 *Fgf4^{c/c}; Fgf8^{c/c}; AP2-Cre* embryo.

seen in the control embryo (Figs. 6B and D). In fact, *Fgf10* expression was still detected at E11 and E11.5 in the most distal tip of the limb bud in double mutants, but the level was greatly reduced (Figs. 6C and E; data not shown). Essentially identical results were obtained for forelimb bud expression of *Fgf10* in *Fgf4^{c/c}; Fgf8^{c/c}; AP2-Cre* embryos (Figs. 6G and H). However, although *Fgf10* transcripts were present in hindlimb buds of *AP2-Cre*-generated double mutants at E10.5, they were not detectable over background at E11–11.5 (Fig. 6H). Correlating with normal limb bud initiation, *Fgf10* expression in *Fgf4^{c/c}; Fgf8^{c/c}; AP2-Cre* embryos at E9.5 appeared only slightly reduced relative to that in controls (Figs. 6A and F).

Although previous models proposed that *Shh* expression was maintained by an *Fgf4/Shh* feedback loop (Laufer et al., 1994; Niswander et al., 1994), *Shh* expression is unaffected by the absence of *Fgf4* in the AER (Moon et al., 2000; Sun and Martin, 2000). In contrast, *Shh* expression is delayed in *Fgf8* mutant hindlimbs (Lewandoski et al., 2000) and decreased in *Fgf8* mutant forelimbs at E11.5, though present at nearly normal levels at E10.5 (Moon and Capecchi, 2000). Therefore, in forelimbs and hindlimbs, it appears that FGF8 is necessary for proper maintenance or initiation of *Shh* expression, respectively, but that other AER FGFs partially compensate in the absence of FGF8. To test whether FGF4 is critical for *Shh* expression in the absence of FGF8, double mutants generated with *RAR-Cre* and *AP2-Cre* were hybridized with a *Shh* probe. *Shh* expression was just barely detectable in double mutant forelimb buds at E10.5 (Figs. 6I, K, and M), but was essentially absent by E11–11.5 (Figs. 6J, L, and N). *Shh* was not detected in the

hindlimbs of double mutants generated with *AP2-Cre* at any stage examined (Figs. 6M and N).

The survival of SOX9-expressing skeletal precursor cells is not specifically compromised in Fgf4/Fgf8 double mutants at E10.5 or E11.5

To determine whether *Fgf4* and *Fgf8* are required for the condensation of limb bud mesenchyme, we examined the expression pattern of *Sox9*. The *Sox9* gene is transcribed in all chondroprogenitor cells (Ng et al., 1997; Zhao et al., 1997), and mesenchymal cells lacking SOX9 are excluded from chondrogenic condensations (Bi et al., 1999). Whole mount in situ analysis showed that *Sox9* transcripts were still detectable in E11.5 *Fgf4^{c/c}; Fgf8^{c/c}; RAR-Cre* double mutant forelimbs though the number of *Sox9*-expressing cells was greatly reduced relative to control (Figs. 7A and B). Therefore, double mutant limb buds retain some capacity to produce condensations of mesenchymal cells. To determine whether the apoptotic cell population detected in double mutant limb buds included mesenchymal skeletal precursor cells, limb sections were double labeled with antibodies that recognize SOX9 and activated Caspase-3. At E10.5, only a few cells destined to undergo apoptosis (positive for activated Caspase-3) were SOX9-positive condensing mesenchymal cells in mutants generated either with *RAR-Cre* or *AP2-Cre* (Figs. 7C–E). At E11.5, in the *Fgf4/Fgf8* double mutant forelimb, SOX9-positive cells were still present and most were not labeled with the anti-activated Caspase-3 antibody or by the TUNEL reaction (data not shown).

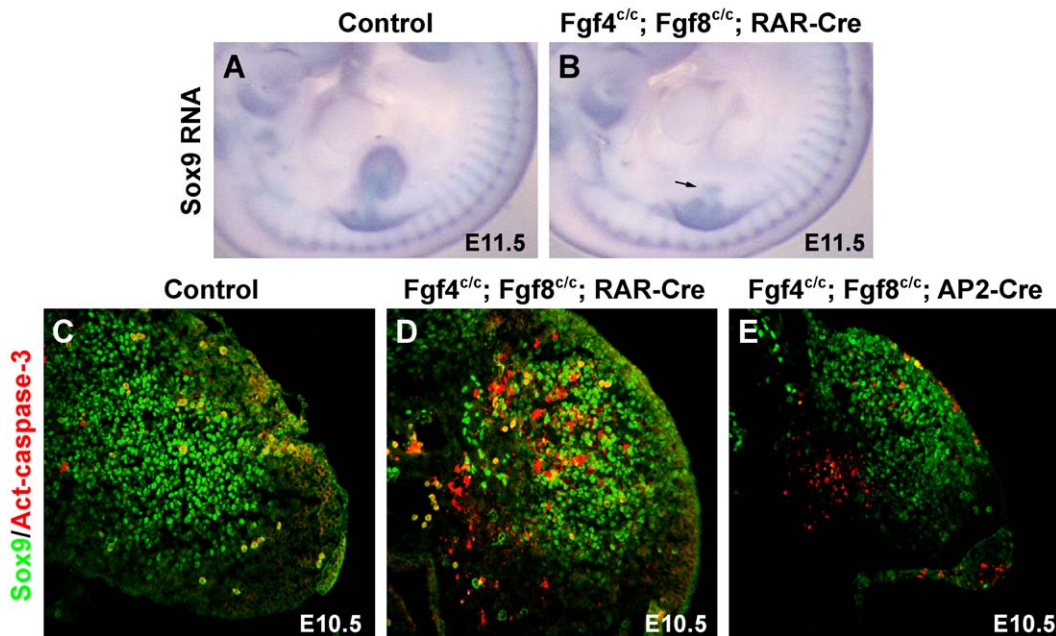


Fig. 7. SOX9-positive skeletal precursor cells are present in limb buds of embryos lacking *Fgf4* and *Fgf8* in the AER. (A and B) Whole mount in situ hybridization of E11.5 control (A) and *Fgf4^{c/c}; Fgf8^{c/c}; RAR-Cre* (B) embryos with a *Sox9* probe. (C–E) Frozen sections of E10.5 (C) control, (D) *Fgf4^{c/c}; Fgf8^{c/c}; RAR-Cre*, and (E) *Fgf4^{c/c}; Fgf8^{c/c}; AP2-Cre* embryos stained with Sox9/9 and anti-activated caspase-3 antibodies.

Discussion

Several roles have been proposed for *Fgf8* and *Fgf4* in limb bud initiation, growth, and patterning. Using tissue-specific inactivation of the *Fgf8* and *Fgf4* genes, we have provided verification for some, but not all, of these functions in the mouse. Because elimination of *Fgf8* from the intermediate mesoderm does not have an effect on limb bud initiation or outgrowth, it is unlikely that *Fgf8* plays any role in limb bud initiation. Due to the difficulty in detecting *Fgf8* expression in the IM, we cannot rule out the presence of a very low level of FGF8 protein production in this tissue in *Fgf8^{cl/c}*; *Lefty2-Cre* mutants. However, evidence from GFP and β -Galactosidase expression patterns strongly suggests that *Lefty2-Cre* is active throughout the mesoderm, and particularly in the IM, at the appropriate stage. In contrast, *Fgf8* and *Fgf4* in the AER are essential for the maintenance of limb bud outgrowth. As previously shown for the hindlimb (Sun et al., 2002), in the absence of both FGF family members, extensive apoptosis in proximal limb bud mesenchyme precludes the formation of any skeletal elements.

While nascent hindlimb buds in *Fgf4/Fgf8* double mutants generated with *Msx2-Cre* are reduced to 75% of normal size (Sun et al., 2002), forelimb buds of double mutants generated with either *AP2-Cre* or *RAR-Cre* did not appear to be smaller than normal. This could represent a difference between forelimbs and hindlimbs, but because we did not make careful measurements, we cannot exclude the existence of a slight reduction in our mutants.

In *Fgf8* limb mutants, a period of extensive apoptosis on day 10 of gestation is followed by partial recovery of limb bud outgrowth. In forelimbs, the ulna and three or four digits are formed even though the humerus, radius, and digit 1 are absent in *Fgf8^{cl/c}*; *AP2-Cre* mutants. Because apoptosis continues and limb bud outgrowth is completely abolished in the absence of both *Fgf4* and *Fgf8*, it appears that *Fgf4* is able to partially compensate for the absence of *Fgf8* in the maintenance of limb bud outgrowth/limb mesenchyme survival. *Fgf9* and *Fgf17*, two other FGF family members expressed in the AER, are unable to substitute for *Fgf4* and *Fgf8* in promoting cell survival, though they may maintain cell proliferation in the distal limb bud mesenchyme (Sun et al., 2002).

Because *Fgf4/Fgf8* double mutants generated using either *RAR-Cre* or *AP2-Cre* fail to form any cartilage precursors that can be detected with Alcian blue distal to the pectoral or both pectoral and pelvic girdles, respectively, it was somewhat surprising that SOX9-expressing cells were detectable in forelimb buds at E10.5 and E11.5. SOX9 is a transcription factor that is essential for chondrocyte differentiation (Bi et al., 1999). Initiation of *Sox9* expression is the earliest known indication that cells have begun the transition to a chondrogenic fate. Therefore, at least before E11.5 in the forelimb, the lack of *Fgf4* and *Fgf8* does not prevent the differentiation of prechondrogenic cells. Instead, it appears that excess apoptosis impedes the production of a

sufficient number of chondrogenic cells to form mesenchymal condensations of an adequate size to progress through the differentiation pathway.

When *Fgf8* is inactivated using *Msx2-Cre*, hindlimbs show a more severe phenotype than forelimbs due to the timing of CRE expression relative to *Fgf8* activation (Lewandoski et al., 2000). Similarly, the phenotype of mice in which *Fgf8* was inactivated using *RAR-Cre* is essentially limited to the forelimbs due to the pattern of *RAR-Cre* expression (Moon and Capecchi, 2000). The phenotype seen in the hindlimbs of *Fgf8^{cl/c}*; *Msx2-Cre* mice is less severe than that seen in *Fgf8^{cl/c}*; *RAR-Cre* forelimbs. Lewandoski et al. (2000) attribute this difference to the longer interval during which *Fgf8* is the only ectodermal FGF expressed in the forelimb bud relative to the hindlimb. While the femur is affected to a similar extent by inactivation using either *AP2-Cre* or *Msx2-Cre*, *AP2-Cre*-mediated recombination causes more severe effects on the zeugopod elements, particularly the fibula, than *Msx2-Cre*. Nevertheless, while a very small remnant of the radius is only rarely present in the forelimb, the fibula was never completely lost from the hindlimb. Thus, while *Fgf4*, with possible contributions from *Fgf9* or *Fgf17*, is able to rescue enough cells to form two zeugopod elements in the hindlimb, these FGFs can only very rarely rescue even a remnant of the radius. This could be the result of timing differences as suggested by Lewandoski et al. (2000) or could be due to differences between forelimbs and hindlimbs in the levels or patterns of *Fgf* expression or even to intrinsic differences in cell survival requirements for forelimb versus hindlimb skeletal precursors. In either case, although hindlimbs are less severely affected than forelimbs in *Fgf8* single mutants, *Fgf4/Fgf8* double mutants entirely lack forelimbs and hindlimbs.

A humerus was never formed in *Fgf8* single mutants generated using *AP2-Cre*, whereas only 70% of *Fgf8^{cl/c}*; *RAR-Cre* specimens completely lacked this element. We infer that the *RAR-Cre* driver is not active early enough to completely eliminate FGF8 production. The remaining *Fgf8* expression must be significantly less than that seen in the forelimbs of *Fgf8*; *Msx2-Cre* mutant embryos, where a brief period of readily detectable *Fgf8* expression in the forelimb allows nearly normal development of the humerus (Lewandoski et al., 2000). In *Fgf8*; *Msx2-Cre* mutants, residual *Fgf8* expression is observed in the ventral ectoderm of the forelimb, where *Fgf8* transcripts first appear, and is eliminated before AER formation. Early expression in the ventral ectoderm is a feature unique to *Fgf8* among the FGF family members expressed in the limb. Therefore, we propose that, before AER formation, FGF8 produced in the ventral ectoderm plays an important role in ensuring the survival of skeletal precursors for the humerus.

In several systems, it has now been established that the role of FGFs is to promote the survival of specific cell populations. In the absence of FGF8, enhanced apoptosis causes elimination of the midbrain, isthmus, and cerebellum

(Chi et al., 2003). Similarly, disruption of the *Fgf8* gene in pharyngeal arch ectoderm results in severe craniofacial and cardiovascular defects due at least in part to increased apoptosis of different neural-crest-derived mesenchymal populations (Frank et al., 2002; Macatee et al., 2003; Trumpp et al., 1999). In the presence of such extensive cell death, it is difficult to determine whether FGFs are also involved in tissue patterning or maintenance of cell proliferation. In fact, whereas a drastic reduction in *Fgf8* levels in the telencephalon causes greatly increased apoptosis, a reduction of only approximately 60% in *Fgf8* hypomorphs did not increase cell death, but revealed a role in regionalization of the neocortex (Garel et al., 2003). The presence of multiple FGF family members also complicates interpretation of functional roles. Therefore, it is not possible at this time to exclude other potential functions in addition to the demonstrated requirement for cell survival.

In conclusion, we have shown that FGFs produced in the AER play a critical role in the outgrowth of the forelimb and hindlimb. The phenotype resulting from loss of *Fgf4* and *Fgf8* is not equivalent to that produced by removal of the apical ectodermal ridge. When the AER is excised from mouse limb buds, extensive cell death of distal limb mesenchymal cells is observed (Sun et al., 2002) and, in the chick, cell proliferation in the distal limb mesenchyme is markedly decreased within 8 h of AER removal (Dudley et al., 2002). Therefore, other factors synthesized in the AER, possibly including additional members of the FGF family, must maintain proliferation and promote cell survival in distal limb bud mesenchyme. Finally, we have provided further evidence that *Fgf8* expression in the IM is not essential for limb bud formation. Other members of the FGF family or as yet unidentified signals from the IM or axial regions may position the limb field within the lateral plate and initiate the process of limb bud formation.

Acknowledgments

We thank Ethan Reichert and Tim Macatee for providing some of the embryos used for this analysis and members of the Moon lab for whole mount in situ probes. We thank Suzi Mansour and Lara Carroll for thoughtful comments on the manuscript, Katia Hatch for assistance with embedding and photography of X-Gal-stained sections, and Gary Gaufo for advice on preparation of cryosections, antibody staining, and confocal analysis.

References

Agarwal, P., Wylie, J.N., Galceran, J., Arkhitko, O., Li, C., Deng, C., Grosschedl, R., Bruneau, B.G., 2003. *Tbx5* is essential for forelimb bud initiation following patterning of the limb field in the mouse embryo. *Development* 130, 623–633.

Bi, W., Deng, J.M., Zhang, Z., Behringer, R.R., de Crombrughe, B., 1999. *Sox9* is required for cartilage formation. *Nat. Genet.* 22, 85–89.

Boulet, A.M., Capecchi, M.R., 1996. Targeted disruption of *hoxc-4* causes esophageal defects and vertebral transformations. *Dev. Biol.* 177, 232–249.

Boulet, A.M., Capecchi, M.R., 2004. Multiple roles of *Hoxa11* and *Hoxd11* in the formation of the mammalian forelimb zeugopod. *Development* 131, 299–309.

Chi, C.L., Martinez, S., Wurst, W., Martin, G.R., 2003. The isthmic organizer signal FGF8 is required for cell survival in the prospective midbrain and cerebellum. *Development* 130, 2633–2644.

Crossley, P.H., Martin, G.R., 1995. The mouse *Fgf8* gene encodes a family of polypeptides and is expressed in regions that direct outgrowth and patterning in the developing embryo. *Development* 121, 439–451.

Crossley, P.H., Minowada, G., MacArthur, C.A., Martin, G.R., 1996. Roles for FGF8 in the induction, initiation and maintenance of chick limb development. *Cell* 84, 127–136.

Dudley, A.T., Ros, M.A., Tabin, C.J., 2002. A re-examination of proximodistal patterning during vertebrate limb development. *Nature* 418, 539–544.

Fallon, J.F., López, A., Ros, M.A., Savage, M.P., Olwin, B.B., Simandl, B.K., 1994. FGF-2: apical ectodermal ridge growth signal for chick limb development. *Science* 264, 104–107.

Fernandez-Teran, M., Piedra, M.E., Simandl, B.K., Fallon, J.F., Ros, M.A., 1997. Limb initiation and development is normal in the absence of the mesonephros. *Dev. Biol.* 189, 246–255.

Frank, D.U., Fotheringham, L.K., Brewer, J.A., Muglia, L.J., Tristani-Firouzi, M., Capecchi, M.R., Moon, A.M., 2002. An *Fgf8* mouse mutant phenocopies human 22q11 deletion syndrome. *Development* 129, 4591–4603.

Garel, S., Huffman, K.J., Rubenstein, J.L., 2003. Molecular regionalization of the neocortex is disrupted in *Fgf8* hypomorphic mutants. *Development* 130, 1903–1914.

Geduspan, J.S., Solorsh, M., 1992. A growth promoting influence from the mesonephros during limb outgrowth. *Dev. Biol.* 151, 212–250.

Johnson, R.L., Tabin, C.J., 1997. Molecular models for vertebrate limb development. *Cell* 90, 979–990.

Kawakami, Y., Capdevila, J., Buscher, D., Itoh, T., Rodriguez Esteban, C., Izpisua Belmonte, J.C., 2001. WNT signals control FGF-dependent limb initiation and AER induction in the chick embryo. *Cell* 104, 891–900.

Laufer, E., Nelson, C.E., Johnson, R.L., Morgan, B.A., Tabin, C., 1994. *Sonic hedgehog* and *fgf-4* act through a signaling cascade and feedback loop to integrate growth and patterning of the developing limb bud. *Cell* 79, 993–1003.

Lewandoski, M., Sun, X., Martin, G.R., 2000. *Fgf8* signalling from the AER is essential for normal limb development. *Nat. Genet.* 26, 460–463.

Macatee, T.L., Hammond, B.P., Arenkiel, B.R., Francis, L., Frank, D.U., Moon, A.M., 2003. Ablation of specific expression domains reveals discrete functions of ectoderm- and endoderm-derived FGF8 during cardiovascular and pharyngeal development. *Development* 130, 6361–6374.

Martin, G., 1998. The roles of FGFs in the early development of vertebrate limbs. *Genes Dev.* 12, 1571–1586.

Meno, C., Ito, Y., Saijoh, Y., Matsuda, Y., Tashiro, K., Kuhara, S., Hamada, H., 1997. Two closely-related left-right asymmetrically expressed genes, *lefty-1* and *lefty-2*: their distinct expression domains, chromosomal linkage and direct neuralizing activity in *Xenopus* embryos. *Genes Cells* 2, 513–524.

Min, H., Danilenko, D.M., Scully, S.A., Bolon, B., Ring, B.D., Tarpley, J.E., DeRose, M., Simonet, S.W., 1998. *Fgf-10* is required for both limb and lung development and exhibits striking functional similarity to *Drosophila* branchless. *Genes Dev.* 12, 3156–3161.

Moon, A.M., Capecchi, M.R., 2000. *Fgf8* is required for outgrowth and patterning of the limbs. *Nat. Genet.* 26, 455–459.

Moon, A.M., Boulet, A.M., Capecchi, M.R., 2000. Normal limb development in conditional mutants of *Fgf4*. *Development* 127, 989–996.

Ng, L.J., Wheatley, S., Muscat, G.E., Conway-Campbell, J., Bowles, J., Wright, E., Bell, D.M., Tam, P.P., Cheah, K.S., Koopman, P., 1997.

- SOX9 binds DNA, activates transcription, and coexpresses with type II collagen during chondrogenesis in the mouse. *Dev. Biol.* 183, 108–121.
- Niswander, L., 2003. Pattern formation: old models out on a limb. *Nat. Rev., Genet.* 4, 133–143.
- Niswander, L., Tickle, C., Vogel, A., Booth, I., Martin, G.R., 1993. FGF-4 replaces the apical ectodermal ridge and directs outgrowth and patterning of the limb. *Cell* 75, 579–587.
- Niswander, L., Jeffrey, S., Martin, G.R., Tickle, C., 1994. A positive feedback loop coordinates growth and patterning in the vertebrate limb. *Nature* 371, 609–612.
- Ohuchi, H., Nakagawa, T., Yamamoto, A., Araga, A., Ohata, T., Ishimaru, Y., Yoshiokam, H., Kuwana, T., Nohno, T., Yamasaki, M., Itoh, N., Noji, S., 1997. The mesenchymal factor, FGF10, initiates and maintains the outgrowth of the chick limb bud through interaction with FGF8, an apical ectodermal factor. *Development* 124, 2235–2244.
- Saijoh, Y., Adachi, H., Mochida, K., Ohishi, S., Hirao, A., Hamada, H., 1999. Distinct transcriptional regulatory mechanisms underlie left–right asymmetric expression of *lefty-1* and *lefty-2*. *Genes Dev.* 13, 259–269.
- Sauer, B., Henderson, N., 1988. Site-specific DNA recombination in mammalian cells by the Cre recombinase of bacteriophage P1. *Proc. Natl. Acad. Sci. U.S.A.* 85, 5166–5170.
- Schwenk, F., Baron, U., Rajewsky, K., 1995. A cre-transgenic mouse strain for the ubiquitous deletion of loxP-flanked gene segments including deletion in germ cells. *Nucleic Acids Res.* 23, 5080–5081.
- Sekine, K., Ohuchi, H., Fujiwara, M., Yamasaki, M., Yoshizawa, T., Soto, T., Yagishita, N., Matsui, D., Koga, Y., Itoh, N., Kato, S., 1999. Fgf10 is essential for limb and lung formation. *Nat. Genet.* 21, 138–141.
- Soriano, P., 1999. Generalized *lacZ* expression with the ROSA26 Cre reporter strain. *Nat. Genet.* 21, 70–71.
- Stephens, T.D., McNulty, T.R., 1981. Evidence for a metameric pattern in the development of the chick humerus. *J. Embryol. Exp. Morphol.* 61, 191–205.
- Stephens, T.D., Roberts, S.G., Marchiando, R.J., Degn, L.L., Hackett, D.A., Warnock, M.A., Mason, M.J., Edwards, D.R., Torres, R.D., Deriemaeker, P.K., Slatosky, J.J., Yingst, D.J., 1993. Axial and Paraxial Influences on the Origin of the Chick Embryo Limb. Wiley-Liss, New York.
- Sun, X., Martin, G., 2000. Conditional inactivation of Fgf4 reveals complexity of signaling during limb bud development. *Nat. Genet.* 25, 83–86.
- Sun, X., Mariani, F.V., Martin, G.R., 2002. Functions of FGF signalling from the apical ectodermal ridge in limb development. *Nature* 418, 501–508.
- Tickle, C., 2003. Patterning systems—From one end of the limb to the other. *Dev. Cell* 4, 449–458.
- Tickle, C., Munsterberg, A., 2001. Vertebrate limb development—The early stages in chick and mouse. *Curr. Opin. Genet. Dev.* 11, 476–481.
- Trumpp, A., Depew, M.J., Rubenstein, J.L., Bishop, J.M., Martin, G.R., 1999. Cre-mediated gene inactivation demonstrates that FGF8 is required for cell survival and patterning of the first branchial arch. *Genes Dev.* 13, 3136–3148.
- Vogel, A., Rodriguez, C., Belmonte, J.C.I., 1996. Involvement of Fgf-8 in initiation, outgrowth and patterning of the vertebrate limb. *Development* 122, 1737–1750.
- Wanek, N., Muneoka, K., Holler-Dinsmore, G., Burton, R., Bryant, S.V., 1989. A staging system for mouse limb development. *J. Exp. Zool.* 249, 41–49.
- Zhao, Q., Eberspaecher, H., Lefebvre, V., De Crombrughe, B., 1997. Parallel expression of Sox9 and Col2a1 in cells undergoing chondrogenesis. *Dev. Dyn.* 209, 377–386.